



THE UNIVERSITY of EDINBURGH
School of Physics
and Astronomy

In Vitro and Computational Approaches for Evaluating Recording Performance of Neuroimplantable Devices

Harrison F. Squires^{1,2}

¹⁾ School of Physics and Astronomy, University of Edinburgh, Edinburgh, UK

²⁾ Department of Physics, University of Melbourne, Melbourne, Australia

(Dated: January 3, 2026)

This literature review explores the common *in vitro* and computational approaches for validating and characterising Micro Electrode Array (MEA) performance for *in vivo* use, highlighting the inconsistencies and limitations in current methods. Widely used techniques, such as Electrode Impedance Spectroscopy (EIS) and *in vitro* electrophysiological recording tests, are critically evaluated alongside less common approaches like individual channel correlation and computational simulations. EIS, while the most commonly adopted method, exhibits significant shortcomings, with promising *in vitro* results often failing to consistently correlate with *in vivo* outcomes. A tenuous link between EIS and Signal-to-Noise ratio (SNR) is identified, implying the need for more reliable techniques. In contrast, *in vitro* electrophysiological recording tests offer clear advantages, such as direct SNR calculation, though they lack rigorous *in vivo* validation. Promising yet underutilised methods, including performance-factor metrics and channel correlation analyses, are also explored. Computational simulations show potential for optimising MEA properties for *in vivo* performance. This review recommends moving beyond a sole reliance on EIS and forms the foundation of the Master's project, which aims to develop a standardised and reliable *in vitro* recording setup to predict the *in vivo* performance of Carbon Cybernetics arrays. This effort is complemented by established electrochemical procedures and final *in vivo* verification.

I. INTRODUCTION

Neuroimplantable devices connect directly to the brain.⁴⁵ This definition covers a myriad of different systems, used to solve a vast number of problems. Successful neuroimplantables include devices used to address hearing loss, through the creation of cochlear implants^{1,2}. Neuroscience groups across the world use them regularly to record and stimulate neuronal signals within the brain.⁵⁰ This allows researchers to better understand the brain and predict or treat diseases such as Parkinson's disease, epilepsy, and paralysis, including quadriplegia^{3–6}. Recent developments have made it possible to achieve single-cell resolution⁷, primarily through reducing the physical size⁵⁵ of electrodes and optimising their material properties^{8–11}.

Micro Electrode Arrays (MEAs) have been developed in various forms for decades, most notably the Utah array that has been commercialised by Blackrock, this acts as the gold standard for MEAs¹². However, MEAs can be⁶⁰

assembled in various configurations, such as planar electrodes or 3D probes. Silicon-based electrodes are the most popular; this is the case for both Neuronexus (planar) and Utah (3D) arrays^{12–15}. Other materials are also considered, such as carbon-based electrodes^{11,16–18}. MEAs typically consist of 16 or more channels.

For many years, the focus has been to make smaller denser MEAs in order to increase the spatial resolution of neuronal recordings. Smaller electrodes have greater spatial specificity⁷, making them more suitable for single-cell measurements. This has introduced several challenges. For example, smaller electrodes exhibit higher impedances, are more prone to mechanical breakage, and experience increased uncertainty in recordings¹⁹. This introduces a need for standardised testing to characterise electrode performance.

Recent advances and investment in the field have been plentiful. Brain-computer interfaces (BCI), devices that facilitate communication between the electrical signals

of the brain and external software²⁰, are becoming increasingly prominent in the private sector. Neuralink²¹, a private neurobiotechnology company headed by Elon Musk, is developing flexible threads that insert into the motor-cortex in an attempt to allow patients with quadriplegia have a better quality of life. As with other neuroimplantable devices, issues are prevalent and right now electrodes implanted in the brain are showing a 39% success rate. Another example, Synchron²² is an American company working in the BCI space; their Stentrode (stent-electrode array) aims to eliminate the requirement for open brain surgery and to allow the use of thought-controlled personal devices. The interest in the field is highlighted by their recent investment of approximately \$75 Million USD. Carbon cybernetics hopes to utilise neuroimplantable devices, specifically carbon-based MEAs, to eliminate epilepsy^{17,23}. With a swathe of research being conducted both publicly and privately, there is a growing need to standardise and ensure the effectiveness of MEA testing techniques before implantation. This will help to better understand the properties of electrodes made from different materials and improve their performance across the research spectrum. A standardised approach will allow for greater quality control, reduce variability, and a focus on key characteristics tailored to specific applications.

This literature review focuses on *in vitro* testing of the recording capabilities of MEAs. *In vitro* testing has been demonstrated to be a cost and time effective way to optimise performance, but requires further refinement to meet the necessary standard for predictability of *in vivo* performance. The following review summarises the current tests in the field and discusses the strategies to improve testing methodologies for MEAs.

II. CURRENT METHODS FOR BENCH-TOP *IN VITRO* TESTING OF ELECTRODES

II.A. Electrode Impedance Spectroscopy

The vast majority of reports in the literature use electrochemical testing as a methodology to characterise and validate MEAs. Among these methods, the most common involves measuring the impedance of electrodes in an MEA, typically using Electrode Impedance Spectroscopy (EIS)^{10,14,15,18,24–26}. Impedance characterises an electrode's ability to resist current flow^{15,25}. It is influenced by geometric surface area, size, conductivity and the interaction with the surrounding electrolyte^{11,17,24}. The electrolyte is the host-solution that confines the electrode, such as brain fluid.

Briefly, this method applies a small AC voltage to a solution through a working electrode. Typically^{24,26,27}, a 10 mV sinusoidal wave is used, with a frequency range of 10 Hz to 30 kHz. The frequency input is varied to determine the frequency dependence of impedance, $|Z(\omega)|$.

By measuring the current at each frequency step, the impedance is calculated using the following relationship:

$$Z(\omega) = \frac{V}{I}$$

A plot of this is shown in Figure 1a. EIS is a mostly standardised procedure^{10,17,18,24,27}.

EIS has been used to predict how good an electrode is with varying degrees of success^{10,13–15,18,19,24,25}. A good electrode should be able to detect signals that are sufficiently distinguishable from noise and for single-unit recordings should be able to be appropriately identify signals as originating from a specific source^{15,19}.

Optimisation can be achieved by comparing electrode properties, to obtain the electrode with the most desirable impedance characteristics^{24,29}. Typically, impedance is to be minimised while maintaining the smallest geometric surface area to maximise spatial resolution. Minimising impedance has been linked to producing high fidelity recordings^{11,15,17,24,28,30–32}, though this is disputed^{10,13,14,25}. Given that impedance and geometric surface area have an inverse relationship, the optimisation of the impedance response of electrodes typically involves the application of surface coatings that improve conductivity while maintaining geometric surface area^{17,18,24,33}.

Lewis et al.²⁴ compared four common coatings applied to Pt-electrodes. They analysed the resulting impedance spectra to quantify how the change in conductivity, induced by the coatings, affects the impedance response. Ultimately, they evaluated how these changes impact the performance of electrodes. Figure 1a shows the typical impedance spectrum of an uncoated Pt-electrode, a nanostructured platinum (nano-Pt), a sputtered iridium oxide film (SIROF) coated electrode and a Poly(3,4-ethylene dioxythiophene)-polystyrene sulphonate (PEDOT) coated electrode. The nano-Pt has increased the effective surface area of the electrode, due to an increase in surface roughness²⁴. SIROF is a thin film that can be applied to electrodes that also has a low impedance due to its relative porosity and rough structure. PEDOT is a conductive polymer³³ with a large electroactive surface area compared to many metals³⁴.

SIROF showed the lowest impedance across all frequencies. However, PEDOT electrodes exhibited the lowest frequency cut-off, this is a measure of the lowest frequency that can be detected to a significant magnitude. Defined formally as the frequency at which the signal is reduced by 3 dB. The cut-off frequency should be set below the signals of interest to prevent frequency-dependent impedance characteristics, such as attenuation, from affecting the results³⁵. In literature, PEDOT is the most common coating used for both metal and non-metal electrodes^{11,16,18,33,34}.

Lewis et al. conducted tests on their MEAs by placing two lateral plate electrodes separated by a fixed distance,

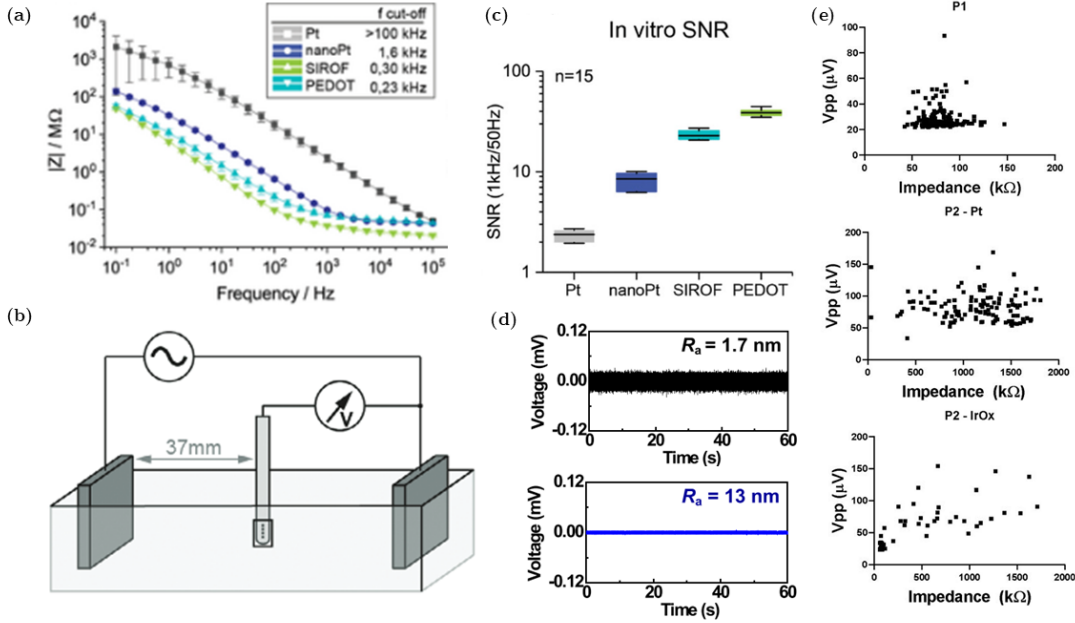


Figure 1 | Plots taken from Lewis et al., Chung et al. and Woepel et al.^{13,24,28}. (a) The effect of different electrode surface coatings (conductivities) on impedance, $|Z|$, plotted against frequency, ω . Coatings compared include Pt, nano-Pt, SIROF, and PEDOT, with SIROF showing the lowest impedance across all frequencies. The bare-Pt electrode has the highest impedance across all frequencies, demonstrating that the addition of any of the surface coating improves impedance performance. Figure taken from Lewis et al.²⁴ (b) Experimental setup from Lewis et al. used to obtain impedance spectrum data²⁴. The schematic shows two parallel plates with an area of 4 cm^2 immersed in PBS (0.01 M), with an MEA in the centre of the container, an AgCl ground electrode, and an AC source. (c) Signal-to-Noise ratio (SNR) at $\omega = 1\text{ kHz}$ for bare Pt electrodes, nano-Pt, SIROF, and PEDOT, illustrating the effect of surface coatings on SNR. PEDOT has the highest SNR, followed by SIROF, nano-Pt and Pt. Figure taken from Lewis et al.²⁴ (d) The effect of increasing the surface roughness on the measured background noise *in vitro*, performed in PBS. A plot of voltage, V , against time, t , is shown for a surface with pores of diameter, R_a , of 1.7 nm and 13 nm respectively. A 12-fold reduction in background noise is determined. The impedance of the electrode and surface roughness are directly linked. Figure modified from Chung et al.²⁸ (e) Comparison of peak-to-peak voltage, V_{pp} , against impedance, $|Z|$, for various electrodes on the last day of testing, highlighting the lack of a trend between impedance and V_{pp} . The lack of correlation between V_{pp} and impedance is consistent across different electrodes. Figure adapted from Woepel et al.¹³

with the MEA of interest positioned in the middle. The 170 plates ensure a quasi-uniform electric field is seen across the homogenous electrolyte. An AgCl electrode was used as a ground, this is a common choice for EIS^{18,24,30,36}. The experimental set-up is demonstrated in Figure 1b. A 195 solution of phosphate-buffered saline (PBS, 0.01 M, pH = 7.4), which is commonly used in *in vitro* tests due to its pH²⁶, which is similar to that of the human body, and its isotonic nature³⁷. Saline is also used commonly^{26,30}.

The Signal-to-Noise Ratio (SNR) quantifies the strength²⁰⁰ of a neuronal signal relative to noise, maximising SNR is desirable. Noise primarily originates from thermal noise, electronic noise introduced by recording equipment and the noise at the electrode-electrolyte boundary¹⁹. Lewis 205 et al. have identified an inverse relationship between impedance and SNR²⁴. This is apparent when considering the plot of SNR against $|Z(\omega = 1\text{ kHz})|$ for different surface coatings. Figure 1c demonstrates that PEDOT has the highest SNR, followed by SIROF, nano-Pt and finally Pt. The 1 kHz impedance value is most com-210 monly referred to as the electrode impedance throughout the literature — as this is the standard for neuronal

recordings^{18,26,30,31,36}.

These results are in accordance with some previous *in vivo* reports^{18,28,32,33,38}. Ludwig et al. found PEDOT improved recording quality over a six week period, impedance was reduced and SNR was improved³². Richie discusses Carbon Fibre Electrodes (CFE), with the application of PEDOT reducing the impedance by up to a factor of 67 and improving the SNR relative to uncoated electrodes¹⁸. Chung et al.²⁸ found that the peak-to-peak voltage of *in vitro* background noise decreased significantly with decreasing impedance. A neural probe was immersed in PBS and the background noise was recorded for 60 s. The impedance was reduced by increasing surface roughness of the electrodes, the diameter of the pores, R_a , were increased from 1.7 nm to 13 nm. The measured background noise went from $74\text{ }\mu\text{V}$ to $6\text{ }\mu\text{V}$ after increasing surface roughness, this is clearly shown in Figure 1d. The *in vitro* results were confirmed by *in vivo* testing, where results showed that lower impedances led to larger signal amplitudes from local field potentials with lower noise, a significant improvement in SNR was achieved.

However, the relationship between impedance and SNR is also disputed in a number of studies. Researchers in the neuroscience space tend to report the 1 kHz impedance to indicate the quality of their electrodes. Several investigations have shown that, during chronic applications, the 1 kHz impedance has no correlation with the recorded local field potentials^{10,13,30}. Baranauskas et al.¹⁵ found that the SNR decreased in the 150–1500 Hz range only, despite a reduction in impedance across the 1–10000 Hz range, following the application of a polypyrrole–CNT coating. However, this observation could not be fully explained using EIS, and no definitive relationship between EIS and noise could be established. Neto et al. found PEDOT-coated gold electrodes demonstrated good adhesion over chronic periods, but during *in vivo* testing the impedance benefits did not significantly improve recording fidelity²⁵. Furthermore, Jiang et al. has shown there to be no relationship between impedance tests and SNR results recorded in primates¹⁰. Indeed, similar observation was documented in rats by Cody et al. and Woepel et al. during *in vivo* studies^{13,14}. This suggests that these trends are not dependent on specific animal models and highlights the limitations of *in vitro* tests in predicting *in vivo* performance.

Woepel et al. demonstrated that impedance and the measured peak-to peak-voltage, V_{pp} from a neuronal source *in vivo* have no clear relationship¹³, this is demonstrated in Figure 1e.

There is suggestion in the literature that low frequency impedances are more effective at predicting MEA performance. Harris et al. found that the 15 Hz range is a more appropriate indicator of *in vivo* performance than 1 kHz^{30,31}. Baranauskas et al., also highlighted the relationship between impedance and SNR to be frequency-dependent, showing the importance of studying the wider EIS spectrum¹⁵. It would be interesting to explore whether other parts of the impedance spectra can provide greater insight into the behaviour of the electrodes *in vivo*. To date, there appear to be no studies utilising the full impedance spectrum of an electrode to predict its efficacy *in vivo*. It is plausible that reducing the frequency required to undergo resistive behaviour could lead to better *in vivo* recordings. Optimising other parameters in the impedance spectrum, such as the frequency cut-off within the range where capacitive behaviour is examined, could prove useful.

Further issues with EIS exist, despite Richie reporting that, while PEDOT does reduce impedance, it is not suitable for chronic applications due to its struggle with binding long-term to CFE¹⁸. This is not predictable through EIS.

Altogether, EIS has demonstrated an inconsistent ability to predict MEA performance for chronic *in vivo* applications, despite promising *in vitro* results. The literature is muddled with contradictory findings, making it difficult to draw clear conclusions solely from EIS. Therefore, fur-

ther exploration of other *in vitro* methods is needed to ensure electrodes are validated in a consistent manner, improving the likelihood of accurately predicting their performance. Exploring a wider frequency range for EIS or adopting alternative measurement approaches could enhance its viability and reliability. These factors make EIS challenging to recommend in its current form as an *in vitro* bench-top test, despite its widespread adoption.

II.B. *In vitro* electrophysiological recording tests

In vitro electrophysiological recording tests have been employed in various studies to evaluate MEA performance. Using cultured cortical neuronal cells is a common approach to measure transient signals *in vitro*^{34,38–42}. A transient response is one that lasts only for a short time^{34,40,43}; action potentials typically last for around 1–10 ms⁴⁴. These setups generally involve placing an MEA in a solution containing neurons, which are then stimulated to produce action potentials. The solution is often PBS or saline^{38,41}. The MEA measures the voltage transients from these *in vitro* action potentials to validate MEA performance.

Recording tests offer additional value in predicting MEA performance, which cannot be achieved solely through EIS, such as *in vitro* SNR calculations^{34,38–42}. Compared to similar *in vivo* tests, these are simplified, requiring fewer considerations and allowing for greater standardisation due to the absence of biological variability, such as brain movement, protein adsorption, variable oxygen levels, tissue heterogeneity, and other neuronal signals³⁰. Noise during recordings poses significant challenges¹⁹, and achieving a thorough understanding of noise in recordings remains an ongoing issue¹⁵.

The commercially available “MEA2100-Systems” is commonly used throughout the literature^{38,39,41,42}. Susloparova et al.⁴¹ validated the use of PEDOT for TiN electrodes, with baseline noise levels reduced from 15 μ V to 9 μ V after applying PEDOT. In agreement, Jones et al. found neural recordings to be significantly improved after the application of PEDOT, with a 1.5-fold increase in measured voltage from cultured cells³⁸, bolstering support for the relationship between impedance and recording fidelity. Similar noise levels were obtained by Boscherini of 9.2 μ V. Successful recordings of spike data from cultured cells was achieved with amplitudes of action potentials being measured at 34 μ V by Boscherini⁴², demonstrating an impressive SNR. Using a commercialised system, electrophysiological *in vitro* recording was used to demonstrate the functionality of MEAs for measuring action potentials. However, the issue is that there is a lack of *in vivo* confirmation of these results so further validation is challenging and the same issues that plague EIS could be present here. Provided further validation can be achieved the system used here is a time-efficient way to verify electrode performance and

gain additional data points with regard to SNR.

Moving to in-house recording systems shifts the primary focus of the studies to their development. Garma et al.⁴⁰ developed their own cost-effective *in vitro* recording system. Cultured cells produced the action potentials recorded by the system and the MEAs were electrically characterised. A high-pass filter of 5 Hz was used, allowing signals above this threshold to pass through without significant attenuation. This filter helps to reduce noise,³⁸⁵ thereby further improving the SNR⁴⁵. The magnitude of the average action potential measured was 127 μ V across 269 channels. These fall within the order of magnitude expected from an action potential and were in lines with those recorded by Aqrawe et al. who measured an average potential of 200 μ V³⁴, the disparity can be accounted for since different MEAs and cell cultures are used. Garma et al.⁴⁰ used 100 μ m planar electrodes, whereas Aqrawe et al.³⁴ used 20 μ m electrodes. An SNR of between 8.9 dB and 17.6 dB, the SNR determined here is broadly in-line with the work of other recording *in vitro* set-ups^{34,39-41}. Furthermore, using similar electrodes *in vivo*, agreement of the results found has been published by Dipalo et al.⁴⁶. Therefore, Garma et al. showed a set-up capable of *in vitro* validation of electrodes. These findings suggest that the recording system is effective at predicting *in vivo* performance.

Aqrawe et al. built on the approach of using an *in vitro* recording system by introducing the use of optics. A Complementary Metal-Oxide Semiconductor (CMOS) camera has been used to take recordings³⁴. In order to obtain a clear optical view of the set-up, voltage sensitive dyes were used. These dyes alter their fluorescent properties in response to changes in membrane potential, enabling the non-invasive imaging of entire neuronal networks⁴⁷. Aqrawe et al. explore the benefit of applying PEDOT^{18,24,33}. Fundamentally the system used is in-line with that of Garma et al. and the commercial systems³⁸⁻⁴². The measured signals are passed through a bandpass filter with an allowed frequency range of 200–1000 Hz, much in the same way as Garma et al. used a high-pass filter⁴⁰.

Aqrawe et al. investigated the short-comings of SNR as a measurement to predict MEA performance³⁴. Highlighting the drawback of being dependent on the distance between the electrode and stimulation source, a larger distance will always lead to a smaller SNR³⁴. The implication here is SNR might not be a reliable indicator of performance. Aqrawe et al. attempt to address this problem³⁴.

Aqrawe et al. introduced the notion of a “performance-factor”, which addresses the bias of SNR that occurs⁴²⁵ based on the separation between the electrode and the action potential³⁴. The “performance-factor” uses the expected voltage incident on the electrode. This is determined by assuming the electrolyte as an infinitely large homogenous medium located at x, y, z with the current⁴³⁰

occurring at x', y', z' . The expected voltage is found using the Method of Images. The solution has a conductivity σ and the action potential instigates a current I . The expected potential is then:

$$V_{\text{expt}}(x, y, z) = \frac{I}{4\pi\sigma\sqrt{(x - x')^2 + (y - y')^2 + (z - z')^2}}$$

The ratio between the expected voltage and the measured voltage defines the “performance-factor”, which can be used to evaluate electrode performance, as expressed by:

$$\text{“performance-factor”} = \frac{V_{\text{expt}}}{V_{\text{real}}}$$

The ideal “performance-factor” is 1.

The SNR from the PEDOT electrode significantly outperformed that of the bare gold electrode, exhibiting an eightfold increase from 2.5 dB to 20 dB. This was in agreement with Jones et al. and Ghazal et al.^{38,39} and further supports the relationship between impedance and SNR^{11,15,17,24,28,30-32}. However, using the optical method, this has been attributed to the larger separation between the action potential measured and the electrode during recordings³⁴. The “performance-factor” only increased three-fold after the application of PEDOT, highlighting the issue with using SNR to quantify performance. Aqrawe et al. used this to demonstrate how the SNR measurements are misleading. This finding suggests that the contradictory reports between EIS and SNR could be a more fundamental problem with SNR, worthy of additional exploration.

Notably, none of the studies citing Aqrawe’s work have adopted the “performance-factor” metric, despite the use of similar methods for *in vitro* recordings being employed by other groups, such as Ghazal et al.³⁹. Ghazal et al. has used *in vitro* recordings in a similar manner to obtain the position of neuronal voltage sources using an algorithm and compare this with the positions seen using an optical microscope³⁹. The approach by Ghazal et al. indirectly highlights the main problem with the “performance-factor” metric: accurately determining an electrode’s position relative to a neuronal source is itself a significant challenge^{34,39}. Currently there is no accurate way of doing this *in vivo*³⁹, limiting the utility of the “performance-factor”. However, this could still be an effective metric *in vitro* given further testing. Nonetheless, Aqrawe et al. did an effective job of exposing potential issues with SNR³⁴, which could imply its misuse.

The work of Garma et al. and Aqrawe et al., along with commercial systems, highlights how *in vitro* recording systems can be used to validate electrode performance^{34,38-42}. The development of low cost custom systems has the advantage of widening accessibility and would improve standardisation as even smaller labs could validate their findings. Recording systems are underutilised in the literature and deserve greater consideration, particularly in light of the challenges posed by

EIS. Further investment and studies would strengthen the methods used for these set-ups and eventually allow for the prediction of performance that is more trustworthy than EIS. However, the papers discussed^{34,39,41,42} often fail to back-up findings with *in vivo* analysis. This leaves uncertainty in the results found. Using the same MEAs *in vivo* would provide evidence for the efficacy of the system, which could then be used to validate future MEAs. In the current form, these tests provide effective methods for testing the hardware's ability to measure action potentials, without needing to consider other biological variations. The ability to optimise performance requires further *in vivo* validation.

II.C. The use of cross-correlation for validation

Swindale and Spacek have also utilised *in vivo* and *in vitro* recordings to predict the functionality of individual electrode channels within an MEA, prior to spike sorting³⁶. The Pearson correlation between nearby channels should fall with respect to distance between the electrode sites. The correlation between signals for channel-pairs was plotted against distance, a curve was modelled and plotted on the same axes with the expected behaviour, Figure 2 demonstrates this. Results are then compared against this expected behaviour to predict issues with the MEA. For every pair of channels the correlation is calculated using the Pearson correlation coefficient for 100,000 random data-points in the recording³⁶. The model of expected behaviour is fitted to show the expected decrease in correlation with respect to increasing channel separation. The function used by Swindale and Spacek is:

$$C(x) = \frac{1 + C_0 ax^\beta}{1 + ax^\beta} \quad (1)$$

Where:

- $C(x)$ is the correlation as a function of distance x
- C_0 , a and β are parameters adjusted through the optimisation to fit observed data

Values that deviate significantly from this, with respect to RMS deviation, d_n , and signed deviation, e_n , are flagged as problematic channels³⁶. This approach effectively revealed mis-localised channels, characterised by large positive e_n values, indicating that the channel map does not accurately reflect the relative spacing of the channels. In addition, it allowed for the discrete identification of non-functional channels, characterised by large negative e_n values and lower than expected correlations, as well as shorted channels, which exhibited higher than expected correlations, approaching a unitary value.

The main advantage for this type of assessment is the time savings for MEAs with large amounts of channels⁵⁰⁵ as it reduces the need for manual inspections. There

are some inherent limitations to the testing performed here, if there is large-scale mislabelling of the relative spatial location of channels the correlation testing will be largely ineffective³⁶. To the best of our knowledge, this technique has not yet been implemented by other groups in their analysis in any published literature, therefore remaining underutilised in the field. This highlights the novelty of the approach and provides an opportunity for further research and implementation by other groups. Additionally, it has the potential to be applied retrospectively to existing datasets^{34,36,39,40}.

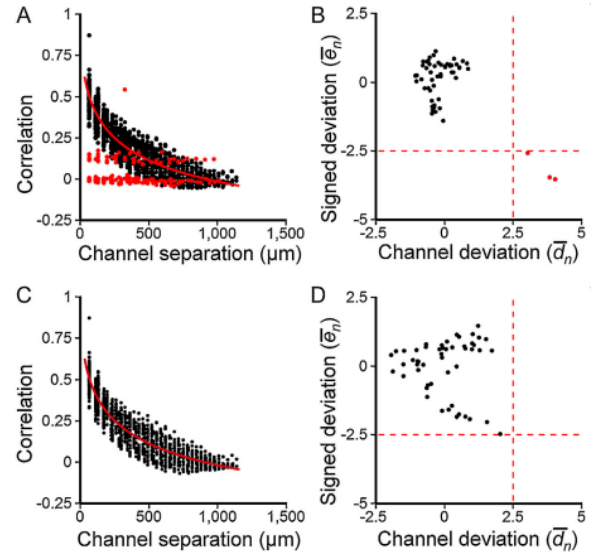


Figure 2 | Plots produced by Swindale and Spacek³⁶. The figure shows a 54-channel electrode correlation with channel separation. The model, described by Equation 1, is represented by the red line, and outliers are marked in red. Panel A shows the Pearson correlation for 1431 unique channel pairs. Panel B presents the plot of e_n against d_n for this data. The dashed lines in Panels B and D correspond to the threshold values of e_n and d_n used to designate outliers. Panel C depicts the data from Panel A with outliers masked, while Panel D shows the outliers masked from Panel B.

III. COMPUTATIONAL MODELLING OF THE IDEAL ELECTRODE FOR NEURONAL RECORDING AND THEIR ELECTRICAL RESPONSES

In addition to *in vitro* tests, simulations can be utilised to determine optimal parameters for the *in vivo* use of MEAs. An ideal electrode maximises SNR across the full frequency band of useful neuronal information¹⁵. In these simulations^{29,43,48,49}, the MEA and surrounding electrolyte are modelled. The electrode-electrolyte boundary is capacitive, and double-layer capacitance at this boundary must be considered⁴⁴. At low frequencies, it is expected to see non-linear distortion of the input signal, with distortion at higher frequencies being less significant due to the system behaving more resistively³⁰.

Simulations have been utilised to compare changes in electrode geometry and factors of the *in vivo* recording system; however, relatively few studies have focused on this topic for recording electrodes^{29,43,48,49}.

Leva et al.⁴³ found that a small electrode of 2 μm shows weak coupling, while a large electrode of 50 μm obscures the EAP and a measures flat response. A radius of $\sim 10 \mu\text{m}$ is determined to be optimal⁴³. This is to the same order of magnitude as electrodes produced by Richie et al. and Massey et al., which are around 7 μm diameter^{16,18}.

Camuñas-Mesa and Quiroga²⁹ highlighted the importance of the amplifiers input impedance, but did not parametrise it during the course of their investigation. They showed that small electrodes of 10 μm have high SNR, but have a limited range spatially, that is they need to be relatively close to the neuron generating the action potential. During *in vivo* applications this would mean the positioning of the inserted electrode would need to be precise. The high SNR of the small electrode of Camuñas-Mesa and Quiroga²⁹ provides confidence of the size of the optimal electrode determined by⁴³. In agreement with Leva et al.⁴³, Camuñas-Mesa and Quiroga showed large electrodes of 300 μm diameter to experience a lower SNR, as a result of the signal averaging across the larger geometric surface area. However, Camuñas-Mesa and Quiroga²⁹ showed the ideal electrode to be 40 μm . The response to EAPs for each electrode diameter over a period of 30 s is shown in Figure 3, demonstrating the effectiveness of the 40 μm in this simulation. This highlights how within these two models there is still disagreement about the precise optimal diameter of an ideal electrode in a MEA. This difference highlights the need for a more thorough investigation *in vivo* in order to verify the simulated results.

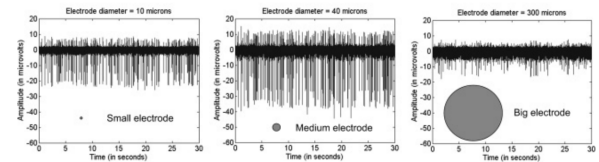


Figure 3 | Plots produced by Camuñas-Mesa and Quiroga²⁹. The plot shows voltage, V , against time, t , for the simulated response of varying electrode sizes: 10 μm , 40 μm , and 300 μm , respectively. The figure highlights that 40 μm produces the clearest signal in response to the EAP.

Leva et al.⁴³ used a parametric sweep of different physical characteristics of the recording electrode to determine the effect of these changes on the measured response. They explored the effect of changing the electrode radius and the amplifier's input impedance by varying its resistance, R_{amp} , or its capacitance, C_{amp} . The amplifiers input impedance is a known contributor of noise during *in vivo* and *in vitro* testing and so is a useful parameter to optimise^{15,25}. It was found that the larger amplifier's impedance, that is, maximising R_{amp} and minimising C_{amp} , led to the largest voltage amplitudes being measured. Impedance, resistance, and capacitance are explicitly linked through Equation 2:

$$Z_{\text{amp}} = \sqrt{R_{\text{amp}}^2 + \left(\frac{1}{\omega C_{\text{amp}}}\right)^2} \quad (2)$$

Malaga et al.⁴⁹ used simulations to in a similar way to Leva et al.⁴³ and found that there is no clear link between changes to impedance of the electrode and the signal quality measured. In agreement with the results obtained through comparisons of *in vitro* EIS measurements and the testing of animal models discussed in section II.A.

In a separate study, Leva et al. used a mixed-mode simulation framework, combining FEM, equivalent circuits, and the Hodgkin-Huxley model to analyse MEAs designed for CMOS-based sensing⁴⁸, this is a similar approach to the previous simulation paper's discussed^{29,43}. Essentially, this paper quantifies the advantage of using active sensors with built in amplifiers and filters, versus

passive sensors⁴⁸. Leva et al. focused on active sensor MEAs with integrated amplification circuits, which provide significantly improved SNR compared to passive⁶⁴⁵ systems.

The paper explores the response for both intracellular and extracellular recordings. Small extracellular signals, even at 100 μ V, require significant post-processing to extract useful information³⁹. Additionally, the challenge of overlapping action potentials from different neurons makes isolating single-neuronal sources difficult.⁶⁵⁰

Leva et al. demonstrate that active sensors achieve higher SNR and larger signal amplitudes than passive⁶⁵⁵ sensors, which do not have onboard amplification⁴⁸. The study also shows that larger electrode diameters improve signal quality, particularly for passive systems, this somewhat disagrees with the Leva et al.'s other paper and Camuñas-Mesa and Quiroga's paper who showed that higher SNR was demonstrated for smaller electrodes²⁹.⁶⁶⁰ Transient voltage responses with different parameters are shown in Figure 4. The paper concludes by recommending active sensors wherever possible and using metal electrodes when passive systems are required.⁶⁶⁵

The models assume the behaviour is non-faradaic, that is there is no chemical change at the boundary^{29,43,48,49}. Capacitive and Inductive effects have been assumed negligible at high frequencies in the work performed by Camuñas-Mesa and Quiroga²⁹, this is appropriate because the electrode-electrolyte boundary acts resistively at sufficient frequencies. The model mostly focuses on high-frequency single neuron responses. Further limitations are the different studies lack of experimental validation, and the simplified treatment of biological environments. Although the trends from this simulation are largely in line with the current literature findings, suggesting simulations could be more widely adopted for the optimisation of physical parameters of MEAs.⁶⁷⁰⁶⁷⁵

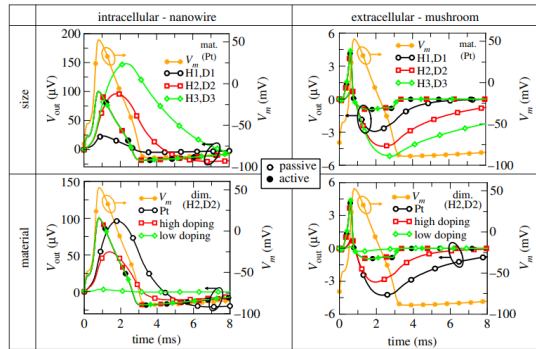


Figure 4 | Plots produced by Leva et al.⁴⁸. The figure shows a plot of peak-to-peak voltage, V_{pp} , as a function of time, t . The transient, short-lived response to an action potential is plotted for different electrode parameters. The left column represents intracellular measurements, while the right column represents extracellular measurements. $H3 > H2 > H1$ and $D3 > D2 > D1$ refer to the height and diameter of the probe, respectively. $V_m(t)$ denotes the action potential waveform.

IV. CONCLUSION AND FINAL THOUGHTS

This literature review has explored the common methods used for testing recording-capable MEAs. The shortcomings of the dominant methods in the field have been addressed, notably the reliance on using EIS for validation of MEA performance and the inconsistency surrounding this throughout the literature. Our primary recommendation is to move away from EIS and focus more on the use of *in vitro* electrophysiological recording tests as the primary method for characterisation. When using EIS, exploring lower frequencies should be given further consideration and an assessment of the entire spectrum should be adopted. Simulations offer an efficient method for predicting changes to electrode geometry, with further *in vivo* validation, they could be effectively used to speed up the production of MEAs.

Current methods are inconsistent and promising methods have been largely unexplored. For example, Swindale and Spacek's cross-correlation approach³⁶ and Aqrawe et al.'s³⁴ comments on SNR. Both of these approaches have the opportunity to improve *in vitro* testing. Further consensus on the best tests is needed in order for consistent findings in MEA development to be comparable across different groups. There is also a need to address the discontinuity between promising *in vitro* performance and *in vivo* testing.

The inconsistent predictive capabilities of *in vitro* testing have posed significant challenges for Carbon Cybernetics, where validating MEA performance has proved challenging. The Master's project focuses on developing an electrophysiological *in vitro* bench-top recording system that will be used in combination with currently employed electrochemical tests aiming to enhance the group's confidence in their MEAs. Underutilised methods will be employed, such as those pioneered by Swindale, Spacek³⁶ and Aqrawe et al.³⁴, among others^{24,30,31}. Comparison between arrays produced commercially will be performed to achieve a control response for comparison of a known effective array.

It is important to note that this literature review deliberately focused on testing electrodes for neuronal recordings. *In vitro* tests for stimulating electrodes are well-documented in the literature and share similarities in impedance testing. However, they also evaluate other properties such as Charge Injection Capacity and Charge Storage Capacity through the use of Cyclic Voltammetry. These aspects, though significant, lie beyond the scope of the current review.

NOMENCLATURE

BCI Brain-computer interface

CFE Carbon Fibre Electrodes

CMOS Complementary Metal-Oxide Semiconductor

| | | |
|-----|----------------------------------|-----|
| EAP | Extracellular Action Potential | |
| EIS | Electrode Impedance Spectroscopy | 760 |
| FEM | Finite Element Method | |
| MEA | Micro Electrode Array | 765 |
| PBS | Phosphate-Buffered Saline | |
| SNR | Signal-to-Noise Ratio | 770 |

REFERENCES

- ¹R. P. Carlyon and T. Goehrung, "Cochlear implant research and development in the twenty-first century: A critical update," *Journal of the Association for Research in Otolaryngology* **22**, 481–508 (2021).
- ²I. Boisvert, M. Reis, A. Au, R. Cowan, and R. C. Dowell,⁷⁸⁰ "Cochlear implantation outcomes in adults: A scoping review," *PLoS One* **15**, e0232421 (2020).
- ³M. Hariz and P. Blomstedt, "Deep brain stimulation for parkinson's disease," *J Intern Med* **292**, 764–778 (2022), 1365–2796
Hariz, Marwan Orcid: 0000-0001-5930-6037 Blomstedt, Patric⁷⁸⁵
Journal Article Review England 2022/07/08 J Intern Med. 2022 Nov;292(5):764-778. doi: 10.1111/joim.13541. Epub 2022 Jul 13.
- ⁴M. Hodaie, R. A. Wennberg, J. O. Dostrovsky, and A. M. Lozano, "Chronic anterior thalamus stimulation for intractable epilepsy," *Epilepsia* **43**, 603–8 (2002).
- ⁵T. J. Foutz and M. Wong, "Brain stimulation treatments in epilepsy: Basic mechanisms and clinical advances," *Biomed J* **45**, 27–37 (2022).
- ⁶T. J. Oxley, P. E. Yoo, G. S. Rind, S. M. Ronayne, C. M. S. Lee, C. Bird, V. Hampshire, R. P. Sharma, A. Morokoff, D. L.⁷⁹⁵
Williams, C. MacIsaac, M. E. Howard, L. Irving, I. Vrljic, C. Williams, S. E. John, F. Weissenborn, M. Dazenko, A. H. Balabanski, D. Friedenberg, A. N. Burkitt, Y. T. Wong, K. J. Drummond, P. Desmond, D. Weber, T. Denison, L. R. Hochberg, S. Mathers, T. J. O'Brien, C. N. May, J. Mocco, D. B. Grayden,⁸⁰⁰
B. C. V. Campbell, P. Mitchell, and N. L. Opie, "Motor neuroprosthesis implanted with neurointerventional surgery improves capacity for activities of daily living tasks in severe paralysis: first in-human experience," *Journal of NeuroInterventional Surgery* **13**, 102–108 (2021).
- ⁷M. Hughes, K. Bustamante, D. Banks, and D. Ewins, "Effects of electrode size on the performance of neural recording microelectrodes," in *1st Annual International IEEE-EMBS Special Topic Conference on Microtechnologies in Medicine and Biology. Proceedings (Cat. No.00EX451)* (2000) pp. 220–223.
- ⁸R. Hu, P. Fan, Y. Wang, J. Shan, L. Jing, W. Xu, F. Mo, M. Wang, Y. Luo, Y. Wang, X. Cai, and J. Luo, "Multi-channel microelectrode arrays for detection of single-cell level neural information in the hippocampus ca1 under general anesthesia induced by low-dose isoflurane," *Fundamental Research* (2023),⁸¹⁵ <https://doi.org/10.1016/j.fmr.2023.05.015>.
- ⁹A. I. Kashkoush, R. A. Gaunt, L. E. Fisher, T. M. Bruns, and D. J. Weber, "Recording single- and multi-unit neuronal action potentials from the surface of the dorsal root ganglion," *Scientific Reports* **9**, 2786 (2019).
- ¹⁰J. Jiang, F. R. Willett, and D. M. Taylor, "Relationship between microelectrode array impedance and chronic recording quality of single units and local field potentials," in *2014 36th Annual International Conference of the IEEE Engineering in Medicine and Biology Society* (2014) pp. 3045–3048.
- ¹¹P. R. Patel, K. Na, H. Zhang, T. D. Y. Kozai, N. A. Kotov, E. Yoon, and C. A. Chestek, "Insertion of linear 8.4 μm diameter 16 channel carbon fiber electrode arrays for single unit recordings," *Journal of Neural Engineering* **12**, 046009 (2015).
- ¹²B. Neurotech, "Utah array," <https://blackrockneurotech.com/products/utah-array/> (2024), accessed: 2024-12-05.
- ¹³K. Woeppel, C. Hughes, A. J. Herrera, J. R. Eles, E. C. Tyler-Kabara, R. A. Gaunt, J. L. Collinger, and X. T. Cui, "Explant analysis of utah electrode arrays implanted in human cortex for brain-computer-interfaces," *Frontiers in Bioengineering and Biotechnology* **9** (2021), 10.3389/fbioe.2021.759711.
- ¹⁴P. A. Cody, J. R. Eles, C. F. Lagenaar, T. D. Kozai, and X. Cui, "Unique electrophysiological and impedance signatures between encapsulation types: An analysis of biological utah array failure and benefit of a biomimetic coating in a rat model," *Biomaterials* **161**, 117–128 (2018).
- ¹⁵G. Baranauskas, E. Maggiolini, E. Castagnola, A. Ansaldi, A. Mazzoni, G. N. Angotzi, A. Vato, D. Ricci, S. Panzeri, and L. Fadiga, "Carbon nanotube composite coating of neural microelectrodes preferentially improves the multunit signal-to-noise ratio," *Journal of Neural Engineering* **8**, 066013 (2011).
- ¹⁶T. L. Massey, S. R. Santacruz, J. F. Hou, K. S. J. Pister, J. M. Carmena, and M. M. Maharbiz, "A high-density carbon fiber neural recording array technology," *Journal of Neural Engineering* **16**, 016024 (2019).
- ¹⁷M. A. Hejazi, W. Tong, A. Stacey, A. Soto-Breceda, M. R. Ibbottson, M. Yunzab, M. I. Maturana, A. Almasi, Y. J. Jung, S. Sun, H. Meffin, J. Fang, M. E. Stamp, K. Ganesan, K. Fox, A. Rifai, A. Nadarajah, S. Falahatdoost, S. Prawer, N. V. Apollo, and D. J. Garrett, "Hybrid diamond/ carbon fiber microelectrodes enable multimodal electrical/chemical neural interfacing," *Biomaterials* **230**, 119648 (2020).
- ¹⁸J. Richie, *Exploration and Realization of Sub-Neuronal Carbon Fiber Electrodes for Recording and Stimulation in the Nervous System*, Ph.D. thesis, The University of Michigan (2024).
- ¹⁹A. Hassibi, R. Navid, R. W. Dutton, and T. H. Lee, "Comprehensive study of noise processes in electrode electrolyte interfaces," *Journal of applied physics* **96**, 1074–1082 (2004).
- ²⁰J. R. Wolpaw, J. D. R. Millán, and N. F. Ramsey, "Brain-computer interfaces: Definitions and principles," *Handb Clin Neurol* **168**, 15–23 (2020).
- ²¹M. Naddaf and L. Drew, "Second brain implant by Elon Musk's Neuralink: will it fare better than the first?" *Nature* **632**, 481–482 (2024).
- ²²B. W. Staff, "Synchron raises \$75m series c led by arch venture partners to advance endovascular brain-computer interface," (2022), accessed: 2024-12-05.
- ²³U. of Melbourne, "Brain implants to predict and prevent seizures," (2023), accessed: 2024-12-05.
- ²⁴C. M. Lewis, C. Boehler, R. Liljemalm, P. Fries, T. Stieglitz, and M. Asplund, "Recording quality is systematically related to electrode impedance," *Advanced Healthcare Materials* **13**, 2303401 (2024).
- ²⁵J. P. Neto, P. Baião, G. Lopes, J. Frazão, J. Nogueira, E. Fortunato, P. Barquinha, and A. R. Kampff, "Does impedance matter when recording spikes with polytrodes?" *Frontiers in Neuroscience* **12** (2018), 10.3389/fnins.2018.00715.
- ²⁶S. F. Cogan, J. Ehrlich, and T. D. Plante, "The effect of electrode geometry on electrochemical properties measured in saline," in *2014 36th Annual International Conference of the IEEE Engineering in Medicine and Biology Society* (2014) pp. 6850–6853.
- ²⁷A. C. Lazanas and M. I. Prodromidis, "Electrochemical impedance spectroscopy—a tutorial," *ACS Measurement Science Au* **3**, 162–193 (2023).
- ²⁸T. Chung, J. Q. Wang, J. Wang, B. Cao, Y. Li, and S. W. Pang, "Electrode modifications to lower electrode impedance and improve neural signal recording sensitivity," *Journal of Neural Engineering* **12**, 056018 (2015).
- ²⁹L. A. Camunas-Mesa and R. Q. Quiroga, "A detailed and fast model of extracellular recordings," *Neural Computation* **25**, 1191–1212 (2013).
- ³⁰A. R. Harris, C. Newbold, D. Stathopoulos, P. Carter, R. Cowan, and G. G. Wallace, "Comparison of the in vitro and in vivo electrochemical performance of bionic electrodes," *Micromachines* **13** (2022), 10.3390/mi13010103.
- ³¹A. R. Harris, B. J. Allitt, and A. G. Paolini, "Predicting neural recording performance of implantable electrodes," *Analyst* **144**, 2973–2983 (2019).
- ³²K. Ludwig, J. Uram, J. Yang, D. Martin, and D. Kipke, "Chronic

- neural recordings using silicon microelectrode arrays electrochemically deposited with a poly(3,4-ethylenedioxothiophene) (pedot) film," *Journal of neural engineering* **3**, 59–70 (2006). ⁸⁷⁰
- ⁸³⁵ ³³M. Ghazal, A. Susloparova, C. Lefebvre, M. Daher Mansour, N. Ghodhbane, A. Melot, C. Scholaert, D. Guérin, S. Janel, N. Barois, M. Colin, L. Buée, P. Yger, S. Halliez, Y. Coffinier, S. Pecqueur, and F. Alibart, "Electropolymerization processing of side-chain engineered edot for high performance microelectrode arrays," *Biosensors and Bioelectronics* **237**, 115538 (2023).
- ⁸⁴⁰ ³⁴Z. Arawe, N. Patel, Y. Vyas, M. Bansal, J. Montgomery, J. Travas-Sejdic, and D. Svirskis, "A simultaneous optical and electrical in-vitro neuronal recording system to evaluate micro-electrode performance," *PLOS ONE* **15**, e0237709 (2020). ⁸⁸⁰
- ⁸⁴⁵ ³⁵J. J. Carr, "Chapter 6 - filtering electronic circuits," in *The Technician's EMI Handbook*, edited by J. J. Carr (Newnes, Woburn, 2000) pp. 65–79.
- ⁸⁵⁰ ³⁶N. V. Swindale and M. A. Spacek, "Verification of multichannel electrode array integrity by use of cross-channel correlations," ⁸⁸⁵ *Journal of Neuroscience Methods* **263**, 95–102 (2016).
- ³⁷K. Kansara and A. Kumar, "In vitro methods to assess the cellular toxicity of nanoparticles," in *Nanotoxicity*, Micro and Nano Technologies (Elsevier, 2020) pp. 21–40.
- ⁸⁵⁵ ³⁸P. D. Jones, A. Moskalyuk, C. Barthold, K. Gutöhrlein,⁸⁹⁰ G. Heusel, B. Schröppel, R. Samba, and M. Giugliano, "Low-impedance 3d pedot:pss ultramicroelectrodes," *Frontiers in Neuroscience* **14** (2020), 10.3389/fnins.2020.00405.
- ⁸⁶⁰ ³⁹M. Ghazal, C. Scholaert, C. Dumortier, C. Lefebvre, N. Barois, S. Janel, M. C. Tarhan, M. Colin, L. Buée, S. Halliez, S. Pecqueur, Y. Coffinier, F. Alibart, and P. Yger, "Precision of neuronal localization in 2d cell cultures by using high-performance electropolymerized microelectrode arrays correlated with optical imaging," *Biomedical Physics & Engineering Express* **9**, 035016 (2023). ⁹⁰⁰
- ⁸⁶⁵ ⁴⁰L. D. Garma, L. Matino, G. Melle, F. Moia, F. De Angelis, F. Santoro, and M. Dipalo, "Cost-effective and multifunctional acquisition system for in vitro electrophysiological investigations
- with multi-electrode arrays," *PLOS ONE* **14**, 1–13 (2019).
- ⁴¹A. Susloparova, S. Halliez, S. Begard, M. Colin, L. Buée, S. Pecqueur, F. Alibart, V. Thomy, S. Arscott, E. Pallecchi, and Y. Coffinier, "Low impedance and highly transparent microelectrode arrays (mea) for in vitro neuron electrical activity probing," *Sensors and Actuators B: Chemical* **327**, 128895 (2021).
- ⁴²M. Boscherini, *Low-cost Neuronal Network Electronic Readout Circuit for Micro-Graphitic Diamond Multi-Electrode Arrays*, Master's thesis, Politecnico di Torino (2022).
- ⁴³F. Leva, C. Verardo, L. J. Mele, P. Palestri, and L. Selmi, "Multi-physics finite-element modeling of the neuron/electrode electrodifusive interaction," in *2022 IEEE Sensors* (2022) pp. 1–4.
- ⁴⁴R. Plonsey and R. Barr, *Bioelectricity: A Quantitative Approach* (Springer, 2007).
- ⁴⁵A. de Cheveigné and I. Nelken, "Filters: When, why, and how (not) to use them," *Neuron* **102**, 280–293 (2019).
- ⁴⁶M. Dipalo, A. F. McGuire, H.-Y. Lou, V. Caprettini, G. Melle, G. Bruno, C. Lubrano, L. Matino, X. Li, F. De Angelis, *et al.*, "Cells adhering to 3d vertical nanostructures: cell membrane reshaping without stable internalization," *Nano letters* **18**, 6100–6105 (2018).
- ⁴⁷C.-B. Chien and J. Pine, "An apparatus for recording synaptic potentials from neuronal cultures using voltage-sensitive fluorescent dyes," *Journal of Neuroscience Methods* **38**, 93–105 (1991).
- ⁴⁸F. Leva, P. Palestri, and L. Selmi, "Multiscale simulation analysis of passive and active micro/nanoelectrodes for cmos-based in vitro neural sensing devices," *Philosophical Transactions of the Royal Society A* **380**, 20210013 (2022).
- ⁴⁹K. A. Malaga, K. E. Schroeder, P. R. Patel, Z. T. Irwin, D. E. Thompson, J. N. Bentley, S. F. Lempka, C. A. Chestek, and P. G. Patil, "Data-driven model comparing the effects of glial scarring and interface interactions on chronic neural recordings in non-human primates," *Journal of Neural Engineering* **13**, 016010 (2015).
- ⁵⁰A. L. Hodgkin and A. F. Huxley, "A quantitative description of membrane current and its application to conduction and excitation in nerve," *The Journal of Physiology* **117**, 500–544 (1952).